sulting in an increase in absorbance at 280 nm of 0.001/min at pH 6.5 at 25 °C in a 3-mL reaction volume containing L-tyrosine).

Glass powder (100–300 mesh) was obtained from Amend Drug & Chemical Co. (New York City) and was washed with 10% nitric acid prior to use; other varieties of glass beads have been successfully used as well.

All chemicals used in this work were obtained from commercial suppliers and were of the highest purity available.

Preparation of the Enzyme. (i) **Acetone Precipitation.** Polyphenol oxidase (20 mg) was dissolved in 6 mL of 50 mM phosphate buffer (pH 7), and the solution was cooled to 4 °C. Then 10 mL of cold (−20 °C) acetone was gradually added with vigorous stirring at 4 °C, and the mixture was left at −20 °C overnight. The precipitated solid was recovered by filtration on a Buchner funnel.

(ii) **Precipitation onto Glass Powder.** Polyphenol oxidase (6 mg) was dissolved in 0.3 mL of 50 mM phosphate buffer (pH 7), and then 600 mg of glass powder was added. The slurry was thoroughly but gently mixed, spread on a watch glass, and left to dry at room temperature with occasional mixing until visibly dry (freely flowing) beads were obtained. Alternatively, the enzyme could be precipitated onto glass powder with acetone by the procedure outlined in (i). The two methods resulted in similar activities of the precipitated polyphenol oxidase in chloroform. Since drying is much faster than acetone precipitation (2.5 vs. about 18 h) and also more convenient, it was used throughout this study for "immobilization" of polyphenol oxidase onto glass powder.

Reduction with Ascorbic Acid. Enzymatically produced 1,2-quinones were reduced to the corresponding catechols by ascorbic acid. Following removal of the enzyme by decantation, 0.5 mL of the chloroform solution was added to 0.5 mL of a 100 mM solution of ascorbic acid in water. The mixture was vigorously shaken with a Vortex mixer for 1 min, and then the aqueous phase was analyzed as described below.

Assays. Several different methods of analysis were employed.

(i) **Spectrophotometry.** Aliquots of the chloroform solution were withdrawn and their absorption spectra measured in the range 360–600 nm. In the case of the enzymatic oxidation of *p*-cresol in chloroform, the maximum absorbance for 4-methyl-1,2-benzoquinone was at 395 nm; the extinction coefficient at that wavelength was determined to be 1.4 $mM^{-1}\cdot cm^{-1}$.

(ii) **GC.** All gas chromatographic measurements were carried out with a 5-m, 530-μm fused-silica capillary column (Hewlett-Packard) (N_2 carrier gas, 30 mL/min; detector and injector port temperature 250 °C) in an appropriate temperature regime.

(iii) **HPLC.** Following the reduction of the enzymatically formed 1,2-quinones with ascorbic acid, the aqueous solutions containing the corresponding catechols were analyzed by HPLC by using a C_{18} reverse-phase μBondapak column (Waters Associates) with an acetonitrile–10 mM phosphate buffer (pH 3) gradient elution system. The products were detected on the basis of their absorbance at 254 nm.

(iv) **Arow's Assay.** Catechols were determined by the colorimetric method.[18] The extinction coefficients at 500 nm were taken from ref 18. Under the assay conditions, monophenols and ascorbic acid do not interfere.

(v) **TLC** analysis on the product of the enzymatic oxidation of *N*-acetyl-L-tyrosine ethyl ester was carried out with silica gel plates and ethyl acetate as a solvent; R_f values were 0.35 for the substrate and 0.25 for the product (ascorbic acid did not migrate).

Stable Simple Enols. 10.[1a] 500-MHz ^1H NMR of Trimesitylethenol and Deuterated Analogues: Complete Signal Assignments and Direct Determination of Equilibrium Steric Isotope Effects from the NMR Integrals of the Isotopomeric Enols

Silvio E. Biali,[1b] Zvi Rappoport,*[1b] and William E. Hull[1c]

Contribution from the Department of Organic Chemistry, The Hebrew University of Jerusalem, Jerusalem 91904, Israel, and Bruker Analytische Messtechnik GmbH, D-7512 Rheinstetten 4, West Germany. *Received December 4, 1984*

Abstract: *E/Z* mixtures of the isotopomers Mes*C(Mes)=C(OH)Mes (**7a/7b**) and Mes*C(Mes)=C(OH)Mes* (**8a/8b**) [Mes = 2,4,6-$(CH_3)_3C_6H_2$; Mes* = 2,4,6-$(CD_3)_3C_6H_2$] were prepared by addition of MesMgBr and Mes*Br to Mes*C(Mes)=C=O. High resolution ^1H NMR at 500 MHz of trimesitylethenol (**5**) and the labeled isotopomers together with NOE data, saturation transfer, and T_1 relaxation times have now led to a complete assignment of the signals for all 15 nonequivalent proton sites in these triarylvinyl propellers. Two OH signals were observed for each isotopomeric pair. The relative integration of the two OH signals and of the methyl signals of the β-ring (cis to α-Mes) and the β′-ring (cis to OH) gave the isotopomeric ratio. Lorentz–Gaussian line-shape transformations, base-line corrections, and several repeated integrations at 500 MHz were used in order to obtain reliable ratios. The *E* isomers **7b** and **8b** (β-ring = Mes*) were present in excess, and the best values of the isotope effects at 302 K are 1.026 ± 0.007 for the ratio **7b/7a** and 1.048 ± 0.027 for **8b/8a**. A statistical analysis showed that the values are significantly different from unity. The isotopomer ratios were ascribed to an equilibrium steric isotope effect where the isomer with the smaller Mes* group cis to the α-mesityl ring is present in a slight excess. The appearance of a separate OH signal for each isotopomer results from slightly different conformations of the labeled derivatives due to the steric isotope effect. This is the first *direct* determination of a steric isotope effect by simple integration of NMR signals.

Steric isotope effects[2] arise from the different effective "size" of isotopic atoms. The covalent C–D bond has a mean bond length which is 0.005 Å shorter than that for C–H, and that for benzene-d_6 is about 3% smaller than that for benzene.[3] A more accurate representation is that steric constraint usually raises vibrational frequencies of hydrogen, leading to a greater zero-point energy. The replacement of hydrogen by deuterium leads to a lower zero-point energy. Hence, putting the deuterium in a constrained rather than the unconstrained situtation decreases the energy more, and the deuterium is favored in the constrained location. This is reflected in both kinetic[2,4] and equilibrium steric isotope effects. Determination of the former is exemplified by

(1) (a) Part 9: Kaftory, M.; Biali, S. E.; Rappoport, Z. *J. Am. Chem. Soc.* **1985**, *107*, 1701. (b) Hebrew University. (c) Bruker Analytische Messtechnik.

(2) Reviews: (a) Carter, R. E.; Melander, L. *Adv. Phys. Org. Chem.* **1973**, *10*, 1. (b) Melander, L.; Saunders, W. H. "Reaction Rates of Isotopic Molecules"; Wiley: Chichester, 1980; pp 189–199.

(3) Bartell, L. S.; Roskos, R. R. *J. Chem. Soc.* **1966**, *44*, 457.

(4) Melander, L.; Carter, R. E. *Acta Chem. Scand.* **1964**, *18*, 1138.

0002-7863/85/1507-5450$01.50/0

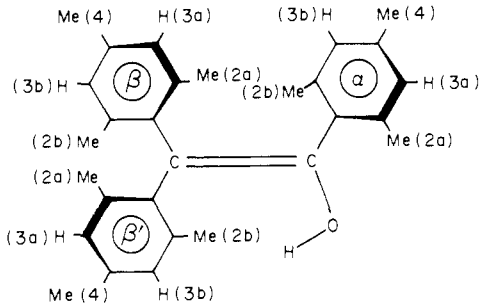

Figure 1. The syn-periplanar propeller conformation and numbering scheme of **5**. Substituents on heavy lines are "up" and substituents on a regular line are "down". For drawing convention see ref 11b.

the observation of Mislow and co-workers that optically active **2** racemizes 1.16 times faster than **1** in heptane at 295 K.[5] Recent advances in NMR instrumentation enabled the study of the "conformational equilibrium steric isotope effect". From the

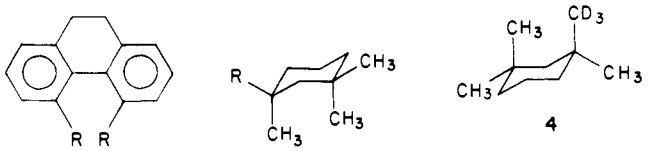

1, R = CH_3
2, R = CD_3

3a, R = CH_3
3b, R = CD_3

$\Delta\delta$(*ax*-Me–*eq*-Me) in the frozen conformation of **3a**, and the $\Delta\delta$ difference at C-3 in the labeled compound under fast **3b** $\rightleftharpoons$ **4** exchange, Anet et al. calculated a conformer ratio $K = [\mathbf{4}]/[\mathbf{3b}]$ of 1.042 ± 0.001 at 290 K.[6] However, owing to incomplete resolution of signals, direct determination of the ratio by intensity measurements under slow exchange was impossible.[6] The presence of an intrinsic steric isotope effect in 1,2-bis(isopropyl)-3,4,5,6-tetrakis(heptadeuteroisopropyl)benzene enabled recently the measurement of the barrier to internal rotation.[7] To the best of our knowledge, no steric isotope effect has been *directly* determined from signal integrals in the NMR.[8] We report here the first case of such a determination.

Results and Discussion

Synthesis of Isotopomeric Enols Having Different or Identical δ(OH) Values. Trimesitylethenol (**5**) which is prepared from the reaction of dimesitylketene and mesitylmagnesium bromide[9] is a highly crowded signal enol[10] where the three rings are arranged in a propeller conformation (Figure 1) in the solid state[1] and in solution.[11] Syn-periplanar and anti-clinal conformations of the OH group in relation to the double bond are in rapid equilibrium even at 200 K, but in relatively weak hydrogen bond accepting solvents the syn-periplanar conformation, where the hydroxyl proton points to the β'-ring (cf. **5**), predominates. For example,

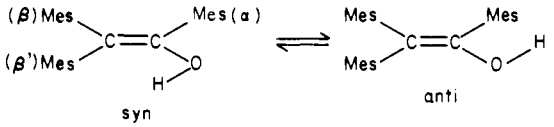

5

Mes = 2,4,6-$(CH_3)_3C_6H_2$

in benzene the population of syn-periplanar is >98%.[12] When a labeled dimesitylketene **6**, where the methyl groups of one mesityl ring [Mes*] are 98.4% deuterated on the average, reacts with mesitylmagnesium bromide, an *E*,*Z* mixture of the isotopomeric enols **7a** and **7b** is obtained. Likewise, when **6** reacts with similarly labeled mesitylmagnesium bromide, an *E*,*Z* mixture of the isotopomeric enols **8a** and **8b** is obtained (eq 1).

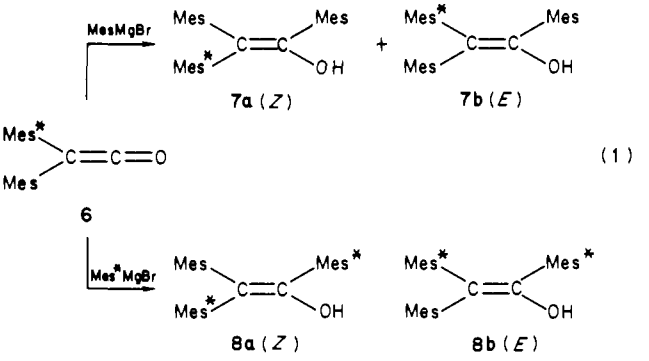

(1)

Mes* = 2,4,6-$(CD_3)_3C_6H_2$

The ^{1}H 300-MHz NMR spectrum of the **7a** + **7b** mixture in C_6D_6 at room temperature shows ca. one-half the normal intensities for the methyl signals corresponding to the β- and the β'-rings. The aromatic proton signal pattern arises from superposition of the unresolved multiplets of the nonlabeled mesityl-ring protons and the resolved doublets ($^4J \approx 2.0$ Hz) of the protons on the labeled ring.[11b] Surprisingly, the OH groups of both isotopomers appear as separate signals, and their reported shift difference $\Delta\delta$(OH) was found to be strongly solvent dependent.[12] For example, $\Delta\delta$(OH) = 7.2, 11.6, 5.9, and 0 ppb[13] in CCl_4, C_6D_6, $C_6D_5NO_2$, and Me_2SO-d_6, respectively. The signal to higher field displayed a slightly higher intensity, and integration gave consistently a ratio in the range of 1.0–1.12, but the value was not sufficiently reproducible and depended on the exact operating conditions of the instrument.

Three different questions were raised at this stage. (a) What is the reason for the splitting of the OH signals? Is it a reflection of an electronic effect or of a steric isotope effect? (b) In the latter case, is it an equilibrium or a kinetic isotope effect? (c) If it is a steric isotope effect, can its magnitude be determined rapidly and accurately by integration of the NMR signals?

In order to answer the first question, we synthesized the sterically closely related pairs of isomers **9a** and **9b**,[12] the pair of

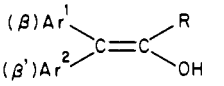

9a, Ar^1 = 4-*t*-Bu-2,6-$Me_2C_6H_2$; Ar^2 = R = Mes
9b, Ar^1 = R = Mes; Ar^2 = 4-*t*-Bu-2,6-$Me_2C_6H_2$
10a, Ar^1 = Mes; Ar^2 = Mes*; R = H or D
10b, Ar^1 = Mes*; Ar^2 = Mes; R = H or D
11, Ar^1 = Ph; Ar^2 = Mes*; R = Mes
12, Ar^1 = Ph; Ar^2 = R = Mes

similarly isotopically labeled but sterically less crowded enol pairs **10a** and **10b** containing either an α-H or α-D, and the mesityl-labeled isotopomer **11** of the known enol **12** by reaction of the corresponding ketene with MesMgBr or with $LiAlH_4$ or $LiAlD_4$.

A ca. 1:1 mixture of **10a** and **10b** showed in the ^{1}H 300-MHz spectrum in C_6D_6 at 293 K only a single singlet when R = D or a single doublet when R = H. Likewise, the OH signal of **11** and **12** appeared at the same position under these conditions.[14] Consequently, it was concluded that the observed splitting for **7** cannot be entirely due to π(Ar)···HO bonding of different strengths when Ar^2 = Mes* (**7a** or **8a**) or Mes (**7b** or **8b**). The presence of this intramolecular hydrogen bond for **5**, **12**, and the unlabeled analogue of **10** in solution was previously deduced from IR

(5) Mislow, K.; Graeve, R.; Gordon, A. J.; Wahl, G. H. *J. Am. Chem. Soc.* **1963**, *85*, 1199; **1964**, *86*, 1733.
(6) Anet, F. A. L.; Basus, V. J.; Hewett, A. P. W.; Saunders, M. *J. Am. Chem. Soc.* **1980**, *102*, 3945.
(7) Siegel, J.; Mislow, K. *J. Am. Chem. Soc.* **1983**, *105*, 7653.
(8) Small steric isotope effects were determined by an ORD method. For a review see: Barth, G.; Djerassi, C. *Tetrahedron* **1981**, *24*, 4123.
(9) Fuson, R. C.; Chadwick, D. H.; Ward, M. L. *J. Am. Chem. Soc.* **1946**, *68*, 389.
(10) For a review on stable enols, see: Hart, H. *Chem. Rev.* **1979**, *79*, 515.
(11) (a) Biali, S.E.; Rappoport, Z. *J. Am. Chem. Soc.* **1981**, *103*, 7350. (b) Biali, S. E.; Rappoport, Z. *Ibid.* **1984**, *106*, 477.
(12) Biali, S.E.; Rappoport, Z. *J. Am. Chem. Soc.* **1984**, *106*, 5641.
(13) ppb = part ber billion.
(14) The experiment was conducted both by comparing the independent spectra of **11** and **12** at the same concentration, or by using a mixture of **11** and **12**.

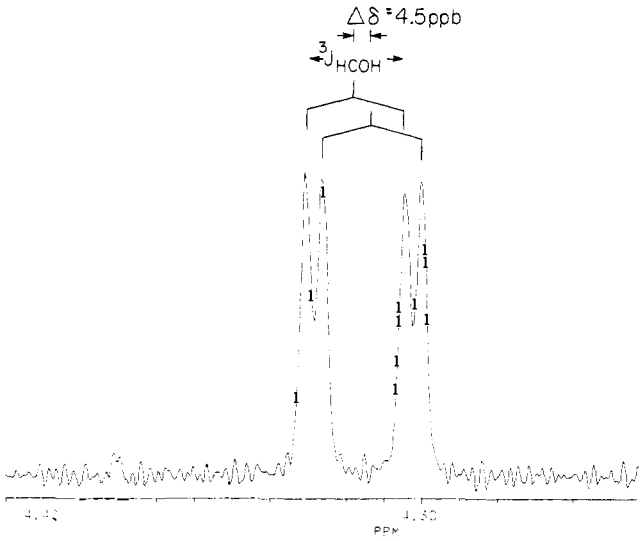

Figure 2. The two OH doublets for the isotopomeric mixture of **10a** and **10b** in C_6D_6 at 302 K; $\Delta\delta$(OH) = 4.5 ppb, $^3J_{HCOH}$ = 13.1 Hz.

studies.[12] A priori, it is expected that the better electron-donating ability of the C–D compared with the C–H bond[15] will increase the π-basicity of the β'-ring, with a consequent shift of the OH of **7a** (and **8a**) to a lower field compared with that in **7b** (and **8b**).[16]

As described below, the assignment of the lower field OH signal to **7a** (and **8a**) in the syn conformation could be made at 500 MHz, where $\Delta\delta$(OH) = 10.8 (11.1) ppb in C_6D_6 at 302 K. Therefore, a sample of **10a/10b** with R = H was reinvestigated under identical conditions. Indeed, a small splitting of the OH doublet into two apparently equal components ($\Delta\delta$(OH) = 4.5 ppb) was detected using techniques of resolution enhancement (Figure 2). The separation was not sufficient for integration purposes. Since any isotope effect that is due to different strengths of hydrogen bonding should be nearly the same in the pairs **7a/7b**, **8a/8b**, **10a/10b**, **11/12**, we conclude that the contribution of such effects to the OH splitting observed for **7** and **8** is less than 5 ppb. However, the basicity of the ring cis to the OH can affect the splitting when the difference in basicity for Ar^1 and Ar^2 is larger: $\Delta\delta$(OH) = δ(OH, **9a**) - δ(OH, **9b**) changes with the solvent from 77 ppb in Me_2SO-d_6 to −81 in $C_6D_5NO_2$.[12] Another possible source of a shift difference that would be similar for all systems is an inherent diamagnetic susceptibility difference for rings bearing Mes or Mes*, leading to different ring currents.

However, we ascribe the large $\Delta\delta$(OH) for the two OH signals for **7** and **8** to *primarily* a steric isotope effect. The X-ray structure of **5** shows that the distances between methyl groups on the same side of the double bond plane (i.e., the 2a or the 2b methyls) are similar or less than the sum of their van der Waals radii.[1] The lower steric interaction between the α and β mesityl rings in **7b** and **8b** compared with that in **7a** and **8a**, respectively (see below), results in a slightly smaller torsional angle of the β-mesityl ring. This effect is partially transmitted to the β'-ring, whose torsional angle also changes slightly. The resulting minor conformational difference between **7a** and **7b** (or **8a** and **8b**) is sensed by the OH group which is in the shielding region of the β'-ring and whose δ value is a sensitive probe of the conformation of the vinyl propeller moiety.

Complete Assignment of the 500-MHz NMR Spectrum of 5. Concerning the third question posed above, we note that, regardless of the reason for the different δ(OH) values, the appearance of a separate OH signal for each isotopomer gives us the opportunity to evaluate directly the isotopomer ratio. As mentioned above, the ratio differs slightly from unity, and we believe (see below) that this is due to a steric isotope effect. This effect is usually small,[3-8] and, in order to establish its existence with certainty and to determine its magnitude, utmost care must be taken to ensure that the small differences in the integration are reliable and reproducible.

At 300 MHz the heights of the two OH signals of the **7a/7b** mixture were different. Since the peaks overlapped, an accurate integration could not be obtained. Under a variety of conditions the less accurate signal heights indicated that the ratio of the signals for the same sample fell in the range 1.0–1.1. However, the heights of the two OH signals of the **8a/8b** mixture were almost the same. Since it appeared that a reliable value could not be obtained at 300 MHz, the ^{1}H spectra of **5** and the **7a/7b** and **8a/8b** mixtures were measured in C_6D_6 at 500 MHz under the most painstaking conditions. The resolution of all nine CH_3 and all six CH signals of **5** was achieved, including considerable fine structure from J coupling.

The improved quality of the spectra at 500 MHz (Figure 3) enabled an accurate integration of the methyl signals which could therefore provide an additional independent measurement of the isotopomer ratio. This requires an unambiguous assignment of the nine methyl signals to the three rings. This will enable the determination of the influence of the steric isotope effect on the δ's at each ring position and on the conformational changes in the molecule. We previously assigned all the methyl signals of **5** in C_6D_6 as belonging to the α or to one of the β- or β'-rings on the basis of synthesis of analogues and of deuterium-labeled derivatives (e.g., **7a/7b**). Pairs of *o*-methyl groups belonging to the same ring were identified[11b] by the saturation transfer method.[17] However, the assignment of groups belonging either to the β- or the β'-ring was based mainly on aromatic solvent-induced shifts (ASIS), on inspection of space-filling molecular models, and on correspondence between chemical shifts in **5** and in the *tert*-butyl analogues **9a** and **9b**. Although the combination of these methods gave a consistent assignment, it was still not unequivocal. We therefore tried to obtain an X-ray structure of **9b**, but although we succeeded to obtain the enthanolate of **9b**, **9b**·EtOH, in >95% purity by crystallization, its crystals were unsuitable for X-ray study. Two additional methods increase our confidence in the assignments previously given. We were able to separate the two isomeric acetates **13a** and **13b**, which are configurationally stable,

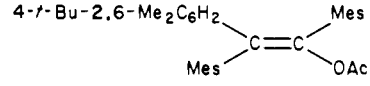

13a

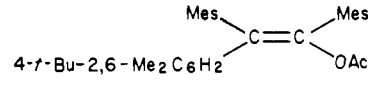

13b

and to determine the structure of the Z isomer **13b**, by X-ray crystallography.[18] The chemical shifts of the *tert*-butyl groups in **13a** and **13b** are nearly identical with those for **9a** and **9b**, respectively, and the structures of **9a** and **9b** were assigned on this basis. The methyl signals in the β-mesityl group of **9b** are in the same positions as those of the methyls in one β-mesityl group of **5**, whereas the signals in **13a** are in similar positions to those of the other β-mesityl group of **5**. This correspondence reinforces the assignments for the β- and β'-methyls given in ref 11b.[19]

At 500 MHz it is possible to confirm and extend previous assignments in an independent manner, without the need for the tedious synthesis and analysis of analogues as described above. As seen in Figure 1 the propeller form of **5** leads to a non-

(15) Halevi, E. A. *Prog. Phys. Org. Chem.* **1963**, *1*, 109.

(16) A significant difference in the strength of the hydrogen bonding to the Mes and the Mes* groups might also be reflected in the frequency of the OH stretching band in the IR. However, the OH stretching bands of a **7a/7b** mixture and of **5** have exactly the same positions and shape and we conclude that the frequency difference between the OH of **7a** and **7b** is much smaller than the bandwidth ($W_{1/2}$ = 20 cm^{-1}).

(17) Forsén, S.; Hoffman, R. A. *J. Chem. Phys.* **1963**, *39*, 2892; **1964**, *40*, 1189; *Acta Chem. Scand.* **1963**, *17*, 1787.

(18) Biali, S.E.; Rappoport, Z., unpublished results.

(19) Comparison of the δ(OH) values for **9a/9b** with those for **7a/7b** could also be used for the assignment. However, because of the opposite order of inductive and hyperconjugative electron-donating effects of aromatic methyl and *tert*-butyl groups, an a priori prediction of the relative basicity of the two rings in **9a** or **9b** is not unequivocal, thus diminishing the value of this analogue.

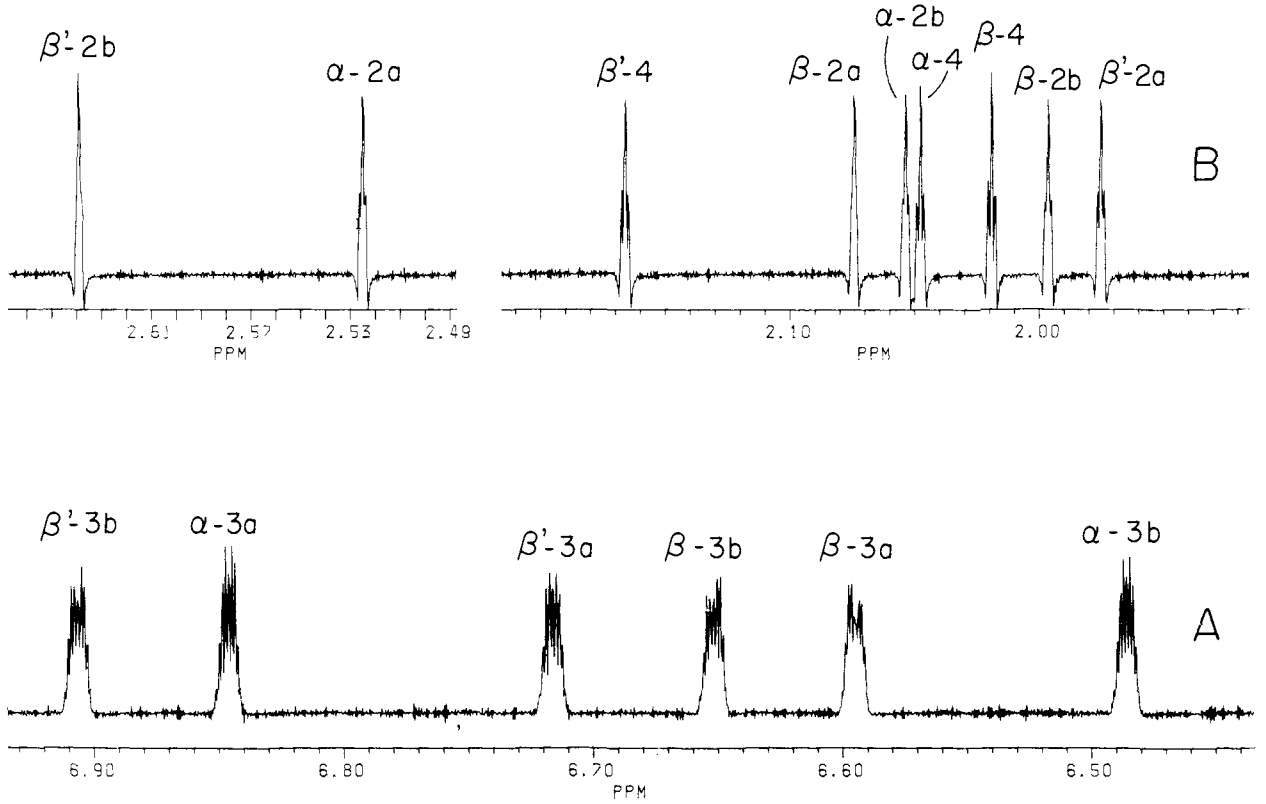

Figure 3. Resolution enhanced 500-MHz ^{1}H NMR spectrum of **5** in C_6D_6 at 302 K. Assignment of the signals is according to Table I.

equivalence of all proton sites which, in principle, should allow for an unequivocal assignment. The pairs of aromatic protons at sites 3a, 3b in each ring are readily detected by homodecoupling, and the 3a, 3b pair for ring α is obvious when comparing **5**, **7**, and **8**. The next step in the assignment process was to identify the methyls by their couplings to neighboring ring protons. Examination of the methyl signals with resolution enhancement (Figure 3) showed a clear distinction between the six ortho methyls (sites 2a, 2b), which appeared as unresolved multiplets with additional fine structure, and three para methyls (site 4) which appear as clearly resolved triplets. The $^4J_{HCCCH_3}$ coupling is ca. 0.62 Hz, but all possible couplings within the aromatic ring system are present. Therefore, the problem was pursued with spin decoupling difference spectroscopy (SDDS). Irradiation of one of the aromatic protons 3a or 3b of **5** gave SDDS responses at all three methyl signals for that ring. However, in each case two methyls gave equal and clearly larger responses than the third methyl, which is on the side of the ring opposite to the irradiated protons (Figure 4). Thus, the structural groupings (*p*-Me, site 4), (*o*-Me 2a, *m*-H 3a), and (*o*-Me 2b, *m*-H 3b) could be assigned. Complementary information was obtained by irradiating the individual methyl signals. The SDDS experiments were performed in such a manner that also generated positive nuclear Overhauser effects (NOE) at neighboring sites and saturation transfer to exchanging sites. Thus, for each ring sites 2a, 2b, and 3a, 3b are being exchanged by the ring-flipping mechanism described in detail in ref 11b. For example, irradiation of proton 3a causes a partial saturation at site 3b, as well as decoupling effects. More puzzling was the observation that irradiation of any signal for one of the β-rings of **5** led to approximately equal transfer of saturation to the related site on the same ring and the corresponding sites on the other β-ring. Such inter-ring transfers were not observed when irradiating α sites. Thus, the *E,Z* isomerization that is of interest here and which causes a slow exchange of the β- and β'-rings was being observed to occur at a rate similar to that for ring flipping, i.e., a rate that is of the order of the relaxation rates $1/T_1$.

Such an effect has not been observed by previous experiments,[11b] and repetition of the experiments at 200 MHz failed to show any inter-ring saturation transfer, as indeed expected since high-temperature dynamic NMR experiments had not resulted in coalescence of β-4 and β'-4 methyl, for example. The barrier to *E,Z* isomerization was estimated to be greater than 25 kcal/mol.[11b] A fresh sample of **5** in C_6D_6 was examined again at 500 MHz, and this time only a very small inter-ring saturation transfer was observed (Figure 5). Since the results described above were obtained with a sample that had stood in the light at room temperature for several days, it appears that trace impurities may have developed which catalyze the *E,Z* isomerization.

In addition to SDDS, a series of NOE difference experiments were performed (see Table II and Figure 5), and the results confirmed the assignments already made. Most importantly, information was also obtained which, in consideration of a space-filling model, allowed a complete stereochemical assignment of all signals. For example, it was found that several *o*-methyl groups generate distinct NOE effects on the OH. The model indicates that the syn conformation of Figure 1 gives OH to methyl distances that increase in the order β'-2b < α-2a < β'-2a < β-2a,2b. The relatively large NOE of 8.5% seen when irradiating at 2.6389 ppm leads to the assignment of β'-2b. The next largest NOE (4.5%) was seen when irradiating 2.5250 ppm which must be α-2a. NOEs of 2.5 and 1.2% give the assignments for β'-2a and α-2b, respectively.

Another important result was the observation of NOEs between *o*-methyls on different rings. For example, β'-2a shows a 1.5% NOE at 2.0744 ppm which must be β-2a which is in van der Waals contact with β'-2a. The β-2a methyl is centrally located between β'-2a and α-2a, giving NOEs of 2.2 and 2.0% to these two sites, respectively. Similarly, β-2b shows NOEs of 2.0% for both β'-2b and α-2b. With these NOE results we have obtained specific stereochemical assignments for each ring and, therefore, it is possible to assign the proton signals for all sites defined in Figure 1 as summarized in Table I, based on measurements of **5** alone. An additional argument made earlier[11b] serves to strengthen the conclusions made here. The methyl groups α-2a and β'-2b are unique in that they point away from the ring interaction regions whereas the other four *o*-methyls all lie in similar shielded environments. Indeed, two methyl signals appear significantly downfield of the others and have been assigned to α-2a and β'-2b.

The NOE difference experiments also provide saturation transfer data for the ring-flipping process and these data along

Table I. ^{1}H NMR Parameters[a] for Trimesitylethenol (**5**) and Deuterated Analogues **7** and **8**

assignments[b]	δ (ppm) for **5**	Δδ (ppb) for **7**	Δδ (ppb) for **8**	$^4J_{3a,3b}$ (Hz)[c]
α-3a-H	6.8460	+0.1 (**7a**, **7b**)		
α-3b-H	6.4862	−0.2 (**7a**, **7b**)		
α*-3a-H			−1.0 (**8a**, **8b**)	1.90
α*-3b-H			−2.0 (**8a**, **8b**)	
β-3b-H	6.6518			
β-3a-H	6.5955			
β*-3b-H		−3.0 (**7b**)	−2.6 (**8b**)	2.075
β*-3a-H		−4.3 (**7b**)	−4.0 (**8b**)	
β′-3b-H	6.9063			
β′-3a-H	6.7162			
β′*-3b-H		−3.2 (**7a**)	−3.3 (**8a**)	2.01
β′*-3a-H		−1.9 (**7a**)	−1.8 (**8a**)	
OH	4.9633	+6.1 (**7a**)	+3.3 (**8a**)	
		−4.7 (**7b**)	−7.8 (**8b**)	
α-2a-Me	2.5250	+0.3 (**7a**, **7b**)		
α-2b-Me	2.0537	+0.2[d] (**7a**)		
		−1.1 (**7b**)		
α-4-Me	2.0477	−0.4 (**7a**, **7b**)		
β-2b-Me	1.9965	−1.4 (**7a**)	−1.4 (**8a**)	
β-2a-Me	2.0744	+0.5 (**7a**)	−0.6 (**8a**)	
β-4-Me	2.0191	−0.2 (**7a**)	−0.1 (**8a**)	
β′-2b-Me	2.6389	−0.9 (**7b**)	−2.2 (**8b**)	
β′-2a-Me	1.9752	−1.0 (**7b**)	−1.7 (**8b**)	
β′-4-Me	2.1658	−0.1 (**7b**)	−0.2 (**8b**)	

[a] Determined in benzene solution at 302 K using 500-MHz ^{1}H NMR (see Experimental Section). The δ values are relative to residual benzene-d_5 defined as 7.170 ppm. The Δδ values represent the δ values for **7** or **8** minus the corresponding δ values for **5**; negative values of Δδ indicate an upfield shift for the analogue. [b] The three mesityl rings are labeled α, β, β′ as described in the text with β cis to α. The superscript * indicates a mesityl ring where CD_3 has replaced CH_3 at positions 2a, 2b, 4. The ring numbering scheme (see Figure 1) defines the nonequivalent ortho positions as 2a,2b: meta = 3a,3b; para = 4. Sites with the same number are interchanged by ring flipping; rings β, β′ are interchanged by rotation about the olefinic bond (*E*,*Z* isomerization). [c] The $^4J_{3a,3b}$ couplings could only be resolved when the methyl groups were deuterated. Couplings $^4J_{23}$, $^4J_{34}$ of ca. 0.62 Hz were observed between *m*-H and neighboring methyls. A $^6J_{H,CH_3}$ is also present in **5** but not resolved. [d] A splitting of the α-2b-Me signal into two components of approximately equal intensity occurs because of van der Waals contact with the β ring which exists in two forms (**7a**,**7b**). No splitting was seen at the more remote α-2a-Me.

with T_1 relaxation times measured on the same sample are presented in Table II. The observed small differences in T_1 for *o*-methyls and meta protons fit well with the stereochemical assignments made. For example, β-2a is located between β′-2a and α-2a and has the shortest T_1 of the three. The proton α-3a is closer to β-2a than is α-3b, and α-3a has the shorter T_1 value. Similar arguments confirm the assignments of 3a, 3b for β- and β′-rings.

Table I also includes information concerning shift differences between **5** and the labeled analogues **7** or **8**, which will be discussed below and serves to further strengthen the assignments already made. The way is now clear for a detailed analysis of the OH and methyl integrals for **7** and **8** for a quantitative determination of the *E*/*Z* equilibrium isotope effect.

Determination of the Steric Equilibrium Isotope Effect for 7 and 8. Table I lists the changes in chemical shifts Δδ for trimesitylethenol caused by introducing CD_3 groups in a β-Mes group (**7**) or in one β-Mes and the α-Mes group (**8**). The largest effect is seen for the OH signal which for **7** splits into two peaks, one downfield (+6.1 ppb) and one upfield (−4.7 ppb) of the original position (4.9633 ppm) seen for **5**. The difference in shifts Δδ(OH) for **7a**/**7b** is 10.8 and 11.1 ppb for **8a**/**8b**, with an upfield displacement of ca. 2.6 ppb relative to **7a**/**7b**. Possible reasons for these absolute shifts will be discussed later. The assignment of the low-field OH signal to the *E* isomer **7a** or **8a** is made based on the analysis of the methyl signals where the populations of β-Mes* and β′-Mes* can be measured directly.

By using Lorentz-to-Gaussian line-shape transformation (resolution enhancement), the two OH signals could be completely resolved in each case (Figure 6). The accuracy of integration

Table II. T_1 Relaxation Times, Saturation Transfer, and NOE Data for Trimesitylethenol (**5**)[a]

signal	T_1 (s)	sat. transfer (%)[b]	NOE (%)[c]
α-3a	2.084 ± 0.011	22.2 (α-3b)	6.9 (α-2a), 7.8 (α-2b + α-4)
α-3b	2.190 ± 0.009	22.4 (α-3a)	3.0 (α-2a), 12.8 (α-2b + α-4)
β-3b	2.134 ± 0.010	23.6 (β-3a)	3.4 (β-4), 6.1 (β-2b)
β-3a	2.186 ± 0.010	22.6 (β-3b)	7.0 (β-2a), 5.0 (β-4), 2.0 (β-2b)
β′-3b	2.084 ± 0.011	21.6 (β′-3a)[d]	6.8 (β′-2b), 7.1 (β′-4), 1.7 (β′-2a)
β′-3a	2.172 ± 0.009	21.6 (β′-3b)	1.8 (β′-2b), 5.5 (β′-4), 7.0 (β′-2a)
OH	2.957 ± 0.010		3.7 (β′-2b), 2.3 (α-2a)
α-2a	1.172 ± 0.011	13.6 (α-2b)	11.5 (α-3a), 4.1 (α-3b), 2.1 (β-2a), 4.9 (OH)
α-2b	1.158 ± 0.010	12.1 (α-2a)[e]	16.0 (α-3b), 8.2 (α-3a), 1.2 (OH), 1.5 (β′-2b)
α-4	1.128 ± 0.015	*e*	13.3 (α-3b), 9.9 (α-3a)
β-2b	1.101 ± 0.004	13.7 (β-2a)	11.7 (β-3b), 4.3 (β-3a), 2.0 (β′-2b), 1.2 (α-2a), 0.8 (OH), 2.0 (α-2b)
β-2a	1.018 ± 0.003	10.6 (β-2b)	11.2 (β-3a), 3.9 (β-3b), 2.2 (β′-2a), 2.0 (α-2a), 0.6 (OH)
β-4	1.252 ± 0.008		9.5 (β-3b), 8.3 (β-3a)
β′-2b	1.106 ± 0.009	11.8 (β′-2a)	10.5 (β′-3b), 3.4 (β′-3a), 8.5 (OH), 1.3 (α-2b), 2.1 (β-2b)
β′-2a	1.147 ± 0.007	12.2 (β′-2b)	12.0 (β′-3a), 4.5 (β′-3b), 2.5 (OH), 1.5 (β-2a)
β′-4	1.136 ± 0.012		9.4 (β′-3b), 9.0 (β′-3a)

[a] In C_6D_6 at 302 K; T_1 measured by nonselective inversion recovery; saturation transfer and NOE were measured from difference spectra. [b] The % saturation at the site in parentheses is given. [c] The % positive NOE at the site in parentheses is given. [d] Additional saturation of 0.9% was observed at sites β-3a, 3b (see Figure 5B). [e] Selective saturation of just one of the two overlapping signals was not achieved; ca. 29% saturation of the other signal was observed.

will be limited by the presence of some impurity signals (ca. 3%) which lie between the main peaks. Since the average deuteration level is 98.4%,[20] we expect the presence of some less deuterated species, e.g., d_7,d_8 species for **7a**/**7b** or d_{16},d_{17} species for **8a**/**8b**, whose signals should fall between those of the major species. Similarly, impurity signals were seen in the aromatic proton and methyl regions of the 500-MHz spectra. Indeed, in preliminary measurements of **7a**/**7b** labeled to an average of 86% the two major OH signals were less resolved,[12] probably since the intensities of the signals of the less deuterated species were larger.

As a test of the accuracy of the data treatment and integration methods employed, the integrals of the six separate aromatic protons for **5** were determined with resolution enhancement. For these protons in the unlabeled material, integrals of 1.00:1.00:1.00:1.00:1.00:1.00 are expected. The observed ratios for **5** (from low to high field) were 1.000:1.008:1.006:1.006:0.991:0.992, where the first value (lowest field proton) was defined as 1.000. Integrals of 0.987:1.003:1.028:1.015:1.010:1.012 were obtained for **7a**/**7b** mixture and 1.000:0.981:1.018:0.993:1.014:0.977 for the **8a**/**8b** mixture. Significantly, the small deviations (due to the aforementioned impurities) from the expected integrals were consistently reduced when the sum of the integrals for the two protons of each ring were compared. In the above experiments the ratios of the aromatic protons in α-, β-, and β′-rings were 1.002:1.000:1.0047 for **5**, 0.995:1.000:0.995 for **7a**/**7b**, and 0.976:1.000:1.006 for **8a**/**8b**. It must be stressed that these integrations were made over the narrowest possible interval for each signal and did not include the ^{13}C satellites. A satellite signal

(20) The presence of a small percentage of the less deuterated isotopomers is corroborated by mass spectral studies. In the mass spectra of **5**, **7a**/**7b**, and **8a**/**8b** the M − 1 and M − 2 peaks are 5 and 1.3% of M for **5**, 3.4 and 16% for **7a**/**7b**, and 30 and 5.3% for **8a**/**8b**. Since the isotope effects in the cleavage of the C–H and O–H bonds are unknown and since high resolution spectra were not measured, the percentages of the d_8 and d_7 and the d_{17} and d_{16} species were not evaluated quantitatively.

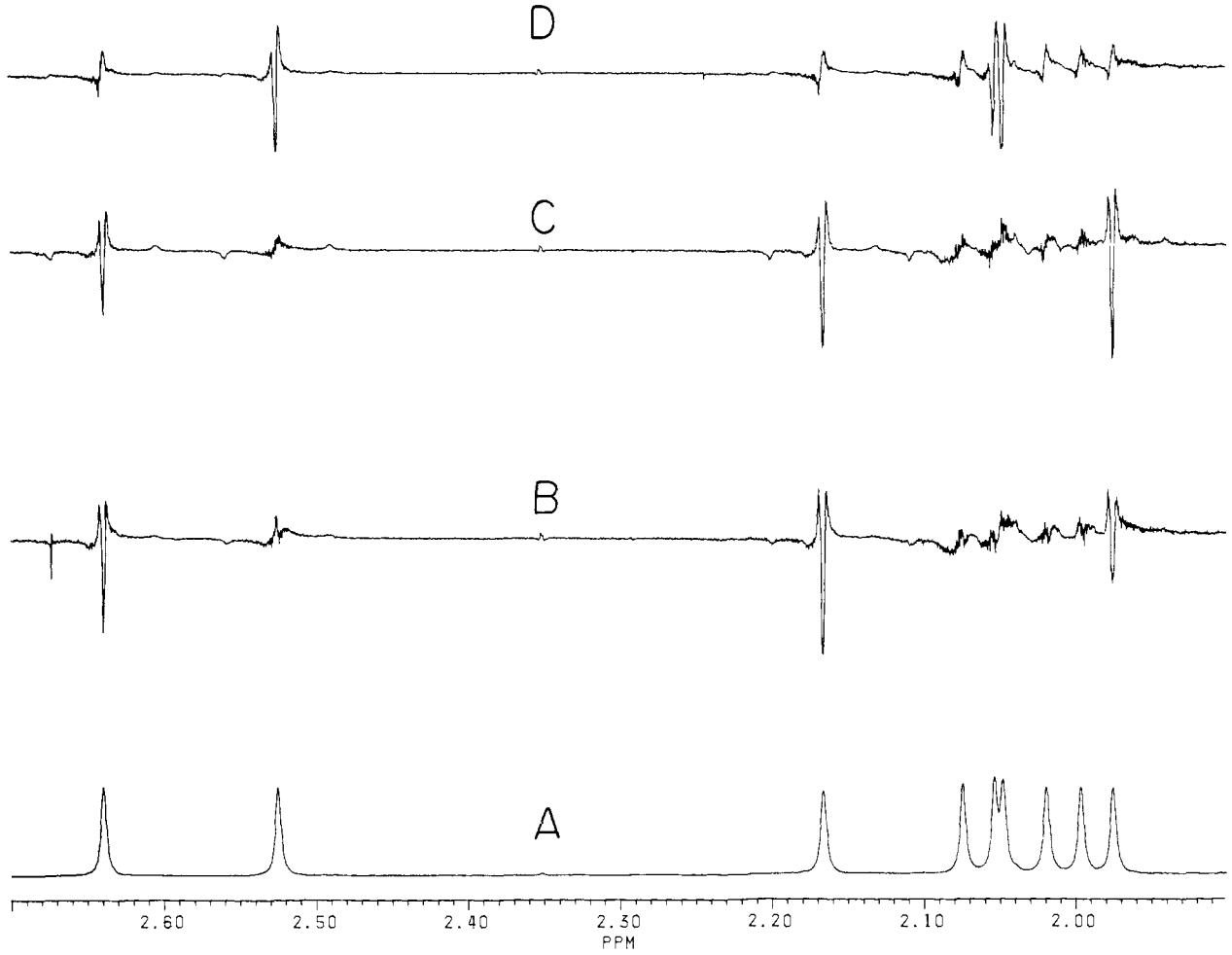

Figure 4. Spin decoupling difference spectroscopy (SDDS) of **5** at 500 MHz. The methyl signal region is shown (cf. Figure 3 for assignment). (A) The "unperturbed" control spectrum without resolution enhancement where the off-resonance irradiation frequency is at 6.775 ppm. (B) The difference spectrum generated by subtracting the on-resonance irradiation experiment (β'-3b-H, 6.9063 ppm) from the control (see Experimental Section). The β'-4-Me and β'-2b-Me signals show a larger effect ($^4J_{H,CH_3}$) $\sim$ 0.6 Hz) than observed for β'-2a-Me. (C) The complementary experiment involves irradiation at β'-2b-Me. (D) A similar experiment irradiating α-3a-H allows the assignment of all α-Me groups.

Table III. Isotopomer Ratios for Labeled Trimesitylethenols

isotopomers	T, K	signal	n^a	E/Z ratios[b,c]	average $(n)^{a,d}$	average $(n)^{a,e}$
7a,7b[f]	302	OH	8	1.026 ± 0.008	1.026 ± 0.007 (11)	1.026 ± 0.006 (15)
			15	1.031 ± 0.009	1.030 ± 0.008 (18)	1.029 ± 0.008 (22)
		Me	3	1.028 ± 0.002		
	283	OH	3	1.026 ± 0.008	1.026 ± 0.004 (4)	
		Me	1	1.025		
8a,8b	302	OH	7	1.072 ± 0.013	1.058 ± 0.026 (10)	1.051 ± 0.022 (18)
			4	1.066 ± 0.023	1.048 ± 0.027 (7)	1.053 ± 0.023 (25)
		Me	3	1.027 ± 0.009		
	283	OH	8	1.046 ± 0.019	1.046 ± 0.018 (9)	
			4	1.046 ± 0.019	1.045 ± 0.019 (5)	
		Me	1	1.040		
	273	OH	4	1.060 ± 0.026	1.057 ± 0.021 (6)	
		Me	2	1.051 ± 0.012		

[a] n = number of different integrations under different conditions. [b] Ratios of **7b** to **7a** or of **8b** to **8a**. For the OH probe the ratio is of the high-field OH to the low-field OH. For the Me probe the ratio is the sum of the three β'-methyls to the three β-methyls. [c] When two values are given, the value with lower n is an average of "best" values, i.e., integrations where the less deuterated impurity species are not included. [d] Average E/Z values for the OH and Me integrations together. [e] Average of the values regardless of the temperature. [f] The ratio was not measured at 273 K since the sample solidified.

from one proton could overlap with the ^{12}C signal of another proton.

Sixteen digital integrations and one intensity ratio at 302 K and three integrations at 283 K of the OH of **7a**/**7b** were conducted under different conditions of data treatment (see Experimental Section). Two less accurate integrations performed without resolution enhancement gave a high **7b**/**7a** ratio of 1.097 ± 0.011 and were discarded. The average of the other values is given in Table III and one trial is illustrated in Figure 6. In some integrations the exact center between the peaks was taken for integrations reset so that a portion of the impurity peaks from less deuterated species was included in the integration of each of the main signals. Integral ratios where the impurity species were omitted gave somewhat more reproducible and consistent results. These are represented in Table III as the average of the "best" integration values. The corresponding ratios for **8a**/**8b** are also given in Table III. Consistently, all the **7b**/**7a** and **8b**/**8a** ratios are larger than unity.

Table IV. Statistical Analysis of the Data for the **7a** ⇌ **7b** and **8a** ⇌ **8b** Equilibria at 302 K

equilibria	$K = [E]/[Z]$	n	std dev	evaluated t^a	confidence[a,b] level, %	$\Delta G°$ cal/mol[c]
7a ⇌ **7b**	1.026	11	0.007	12.32	>99.99	−15.4 ± 4.1
8a ⇌ **8b**	1.048	7	0.027	4.70	>99.83	−28.1 ± 15.7

[a] t values were calculated by standard methods. Confidence levels were obtained from the usual t table (Meyer, S. L. "Data Analysis for Scientists and Engineers"; Wiley: New York, 1975; p 274). [b] For the question whether there is a significant difference between the E/Z ratio and 1.000. [c] Calculated from the equation $\Delta G° = -RT \ln K$; the E isomer has the lower free energy.

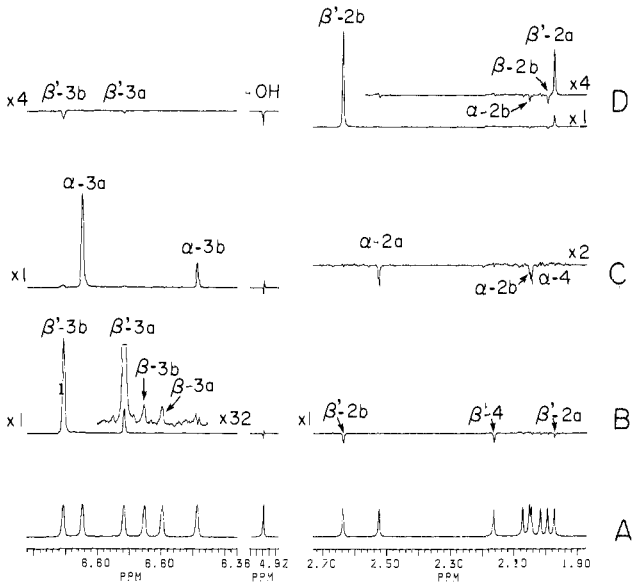

Figure 5. The 500-MHz NOE difference spectra of **5** in C_6D_6 at 302 K (freshly prepared). The aromatic, hydroxyl, and methyl regions are plotted separately. (A) The reference spectrum in which the decoupling frequency was set at about 4.0 ppm. Each group of signals is plotted to give the same signal height. (B) Difference spectrum obtained by substracting the spectrum with on-resonance presaturation of β'-3b from the reference spectrum. Thus, the saturated spin gives a large positive signal whose integral can be defined as 100%. Transfer of saturation gives smaller positive signals. Positive NOE effects appear as negative signals in this mode of presentation. (C) Difference spectrum for irradiation at α-3a. The decoupler power setting was higher than is optimal so that a small amount of saturation also occurred at β'-3b. (D) Difference spectrum for irradiation at β'-2b methyl, showing the significant NOE for the OH signal.

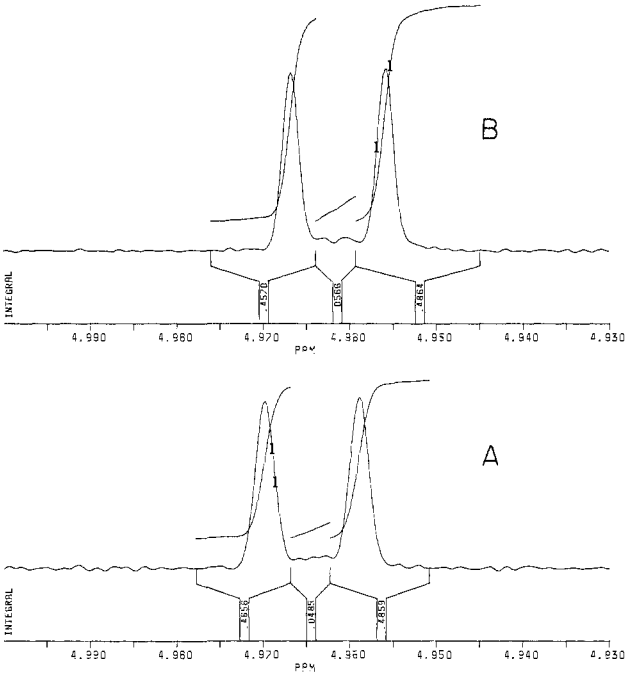

Figure 6. Resolution-enhanced, 500-MHz ^1H NMR spectra of the OH region of **7a**/**7b** (A) and **8a**/**8b** (B) at 302 K in C_6D_6. Note the small unresolved peaks for the less deuterated species between the two main signals. The ratios determined by integration for this particular trial by omitting the central region are **7b**/**7a** = 1.043, **8b**/**8a** = 1.064. Dividing the central region equally between the two peaks gives ratios **7b**/**7a** = 1.041, **8b**/**8a** = 1.060.

The **7b**/**7a** and the **8b**/**8a** ratios from the integration of the β- and β'-methyl groups are also given in Table III. In each case the sum of the integrals for β' was divided by the sum for β. There are some small impurity signals and the unobserved ^{13}C satellites so that a careful baseline correction was necessary for each signal. Again, the accuracy of the integration was tested by integration of the corresponding signals in **5**. Luckily, the only two signals which were not completely resolved and required integration together belong to the α-ring. The relative integrations (from low to high field) were 1.000:0.988:1.009:0.996:2.002:1.014:1.011-:1.011, and the sum of the integration of the methyls of the α-ring to the sum of the β- and the β'-rings is 0.495. The corresponding ratio for **7a**/**7b** was 0.992, while the calculated value on the basis of 98.4% deuteration is 0.984. Consequently, we feel confident that the absolute accuracy of integration ratios for the labeled compounds is limited only by impurities and that the integrals are accurate measures of the isotopomer ratios, to within ca. 1% for **7** and ca. 2% for **8**.

Nature and Magnitude of the Steric Isotope Effect. Table III and the Student t tests of Table IV show unequivocally that the E/S isotopomeric ratios differ from unity. The consistency between the ratios based on the OH and the β/β'-Me signals of **7** is gratifying. For **8** a higher level of impurity peaks reduced the accuracy of the measurements. In particular, the discrepancy between OH and Me E/Z values at 302 K was explained by lowering the temperature. The resultant sharpening of the OH signals and slight shifts led to the uncovering of an additional impurity signal. No temperature effect could be observed for **7** while for **8** the methyl integrals hint at a slight increase in E/Z at lower temperatures, but the OH results do not allow confirmation. Hence, only average values of E/Z will be considered. We ascribe the average **7b**/**7a** or **8b**/**8a** ratios to a steric isotope effect. The ratio is higher than unity since a CD_3 group is sterically slightly smaller than a CH_3 group[2,5,6] and hence Mes* is slightly smaller than Mes. Since the largest steric interaction in the system is between the *o*-methyl groups, the isomers whose CD_3 groups occupy the most crowded (β) position are preferred at equilibrium, as found with other systems.[2,6] Consequently, **7b** with the α-β* and β'-β* interactions will be present in excess over **7a** at equilibrium. Similarly **8b** with α*-β* and β'-β* interactions is favored over **8a**.

However, regardless of the detailed mechanism for the formation of **7a**/**7b** and **8a**/**8b**, part of these interactions are also present in the transition state, since the two faces of the π-orbital attacked by the Grignard reagent are in a diastereotopic environment. Consequently, the isotopomers will be formed at different rates, and the observed population differences might reflect a kinetic isotope effect.

Whether the effect is a kinetic or equilibrium isotope effect depends on the stability of the isotopomers to mutual isomerization during their formation or during the measurements. Although the enolate ion formed in the Grignard reaction was neutralized by NH_4Cl in order to avoid strong acidic conditions, isomerization of the nucleophilic double bond could take place under slightly acidic conditions, by addition of a proton. Whereas the steric crowding will reduce the rate of proton addition to the double bond, some cis interactions will be relieved in the intermediate cation,

and this may serve as a driving force for the process. Moreover, a thermal isomerization, as found for crowded doubly bonded systems,[21] is also possible.

Studies related to the stability of the double bond to isomerization indicate that the effect is an equilibrium steric isotope effect. When a 95:5 mixture of **9b** to **9a** is dissolved in different organic solvents at room temperature, a **9b**/**9a** equilibrium mixture is obtained after a short time. For example, when the sample is dissolved in C_6D_6 the equilibrium mixture of [**9b**]/[**9a**] = 1.34 is already present at the first measurement after a few minutes. The isomerization process is much slower in $CDCl_3$. Although the isomerization mechanism is unknown, it is certain that the **7a**/**7b** and **8a**/**8b** samples, which were crystallized from hot EtOH and which were dissolved many times in C_6D_6 for the various measurements which took many hours, isomerized to a stable mixture in a similar way.

As mentioned above, a $\beta \rightleftharpoons \beta'$ topomerization for **5** was also directly detected in a sample that had stood for several days. In the saturation transfer experiment, irradiation of site 2a (or 3a) of the β- or the β'-ring resulted in a decrease in the signal intensities at site 2b (or 3b) of the same ring as well as both 2a,b (or 3a,b) of the other ring. Consequently, the *o*-Me groups of the β and β' rings are involved in dynamic processes (ring flipping and $E \rightleftharpoons Z$ isomerization) which cause their magnetic environments to be interchanged.

The saturation transfer and T_1 data of Table II can be analyzed for the rate of ring flipping and *E*,*Z* isomerization of **5** at 302 K in C_6D_6 (freshly prepared). Using the formalism of Noggle and Schirmer[22] and the simplification that exchanging sites have nearly equal T_1 values, we define a relaxation rate $R = (1/T_1) + k$, where $1/T_1$ is the spin–lattice relaxation rate for a given site in the absence of exchange and k is the first-order exchange for two sites with equal populations. For a nonselective inversion–recovery T_1 experiment the *Z*-magnetization I_z for each site relaxes to its equilibrium value I_0 as $I_z = I_0\{1 - 2\exp[-(R - k)t]\} = I_0\{1 - 2\exp(-t/T_1)\}$, i.e., a single exponential with time constant T_1. For the difference spectra used to investigate saturation transfer, the fractional saturation f transferred from one irradiated site to the exchanging site is $f = (I_0 - I_z)/I_0 = k/R$, which can be rearranged to give $k = f/[T_1(1 - f)]$. The data in Table II give a rate constant for concerted ring flipping of $k_{flip} = 0.13 \pm 0.01$ s^{-1} for all sites. The previously determined $\Delta G^{\ddagger}$ for ring flipping of 18.4 kcal/mol in $C_6D_5NO_2$[11b] from coalescence measurements suggests a value of $k_{flip} = 0.29$ s^{-1} at 302 K, which is consistent with the directly measured value of this work. As seen in Figure 5B a very small amount (0.9%) of saturation transfer from β'-3b to β-3a,3b was observed, leading to a limit for the isomerization rate of $k_{EZ} \lesssim 4.2 \times 10^{-3}$ s^{-1} with $\Delta G^{\ddagger} \geq 20.9$ kcal mol^{-1}.

The hydroxyl signals of **7** and **8** showed line widths at 302 K significantly larger (3.1 and 2.1 Hz, respectively) than that observed for **5** (0.56 Hz). This could be partly due to the $E \rightleftharpoons Z$ isomerization, but the rate constant derived above is far too small to give any line-width contributions. The syn–anti isomerization and exchange with small amounts of water in the samples (observed for **3**) could be responsible for the observed hydroxyl line widths.

In addition to the steric contribution to the isotopomer ratios two other interconnected contributing factors should be discussed, a polar and a hydrogen-bonding component. The combination of these effects can give a significant E/Z ratio as shown by the fact that a change of a single *p*-Me of **5** to *p*-*t*-Bu group leads to an equilibrium (**9b**/**9a**) ratio of 1.34. We believe that this is due to the increased extent of electron donation by the *p*-*t*-Bu group compared to the *p*-Me substituent (more negative Hammett σ_p for *t*-Bu) which results in a stronger basicity of the β'-ring containing *t*-Bu for isomer **9b**. The strength of the OH···$\pi(\beta'$-Ar) hydrogen bonding was estimated as ca. 1 kcal mol^{-1},[12] and a small fraction of this value is sufficient to account for the observed isomer ratio. The much smaller difference in the inductive/hyperconjugative electron donation between CH_3 and CD_3 and the fact that $\Delta\delta$(OH) is only 4.5 ppb for the **10a**/**10b** pair suggest that this effect for **7a**/**7b** or **8a**/**8b** is smaller than the steric effect. In fact, an increase in π(Ar) basicity for CD_3 would favor the *Z* isomer and works against the steric effect. The difference in $\Delta G°$ value for the equilibrium protonation of $C_6D_5NH_2$, where a charge is formed and the isotope effect should be *much* higher than for the hydrogen-bonding effect in our neutral system, is 31 cal mol^{-1},[15] i.e., twofold higher than in our case. An unequivocal evaluation of the contribution of hydrogen bonding might be obtained by observing the methyl signals in the isotopomeric trimesitylethylenes where an OH···π(Ar) bond is impossible.

Inspection of Table III shows that the **7b**/**7a** ratios determined from the OH and the Me signals are remarkably similar, that the $K_{E/Z}$ values change only slightly even if the less accurate intergrations are included, and that the temperature effect on the ratios is negligible. The best average values are 1.026 ± 0.007 ($n = 11$) at 302 K and 1.026 ± 0.006 ($n = 4$) at 283 K, and the corresponding $\Delta G°$ values are -15.5 ± 4.1 and -14.5 ± 3.3 cal mol^{-1}. Statistical analysis shows that the values are significantly different from unity (Table IV). Comparison with literature values of equilibrium (conformational) steric isotope effects shows that these were mostly measured for methyl-substituted cyclic derivatives and they are generally <25 cal mol^{-1}.[6,8,23a-c]

A very high value of a steric isotope effect was reported for the reaction of Me-labeled, 2,6-dimethylpyridine with BF_3,[23d] but the error in the value is appreciable. Consequently, our values are in the range found for related systems. In contrast, most values of the kinetic isotope effects are somewhat higher, being 81–120 cal mol^{-1}.[4,5,24]

If we consider the steric interactions in a simplistic way it would be expected that the isotope effect for **8b**/**8a** should be the same as that for **7b**/**7a**, since the only difference between the two systems is the labeling of the α-mesityl group in *both* isotopomers of **8**. In other words, the $\Delta G°$ for $\alpha \leftrightarrow \beta$ vs. $\alpha \leftrightarrow \beta^*$ steric interactions might be the same regardless of whether the α-ring is deuterated or not. However, the "best" $K_{E/Z}$ values for **8** (1.048 ± 0.027 at 302 K, 1.045 ± 0.019 at 283 K, and 1.057 ± 0.021 at 273 K; $\Delta G° = -28.3 \pm 15.7$, -24.9 ± 10.4, -30.3 ± 11.0 cal mol^{-1}, respectively) are higher than the values for **7** by about 1 standard deviation. The increased error for **8** reflects the fact that since both mesityl groups are 98.4% deuterated on the average the percentage of impurity species is larger than for **7a**/**7b**. Thus, the accuracy of the intergration is limited by the presence of unidentified signals that partially overlap with signals of interest. Hence, we note that the larger $\Delta G°$ for **8b**/**8a** is not statistically secure, but it cannot be ruled out that subtle cooperative effects may cause an increase in $K_{E/Z}$ when the α-ring is deuterated.

Analysis of Chemical Shift Differences. The chemical shift differences summarized in Table I are of considerable interest but are difficult to analyze. Nearly all shifts are upfield when Mes* replaces Mes as expected for the usual inductive effects of the C–D vs. C–H bond. However, in nearly all cases the $\Delta\delta$ values are different for the two sides of a given aromatic ring (i.e., 3a vs. 3b, 2a vs, 2b). For example, for Mes* in the β position (**7b**) the 3a and 3b protons are shifted −4.3 and −3.0 ppb, respectively, relative to **5**. For Mes* in the β' position (**7a**) 3a and 3b shift −1.9 and −3.2 ppb, respectively. Minimal shifts were observed for 3a, 3b sites in the α ring for **7a**/**7b**, where the two isotopomers could not be observed separately. The shifts for α-3a,3b in **8a**/**8b** are −1.0 and −2.0 ppb. The unique stereochemical identity for each of the six aromatic protons is reflected in the individual shift effects, suggesting an intrinsic steric isotope effect.[25] In going

(21) Sandstrom, J. *Top. Stereochem.* **1983**, *14*, 84.
(22) Noggle, J. H.; Schirmer, R. E. "The Nuclear Overhauser Effect"; Academic Press: New York, 1971; Chapters 6 and 7.
(23) E.g.: (a) Baldry, K. W.; Robinson, M. J. T. *J. Chem. Res. M* **1977**, 1001; (b) Baldry, K. W.; Robinson, M. J. T. *Tetahedron* **1977**, *33*, 1663. (c) Lee, S. F.; Barth, G.; Djerassi, C. *J. Am. Chem. Soc.* **1981**, *103*, 295. (d) Brown, H. C.; Azzaro, M. E.; Koelling, J. G.; McDonald, G. J. *Ibid.* **1966**, *88*, 2520.
(24) Dahlgren, L. *Acta Chem. Scand.* **1969**, *23*, 504; **1970**, *24*, 663. Sherrod, S. A.; de Costa, R. L.; Barnes, R. A.; Boekelheide, V. *J. Am. Chem. Soc.* **1974**, *96*, 1565.

from **7** to **8** we find very little effect on sites 3a, 3b in the β'-ring and small effects in the β-ring.

The methyl signals also show interesting effects. For example, in **7a**/**7b** the α-2a-Me moves slightly downfield +0.3 ppb while α-2b-Me splits into two signals of half intensity. One signal shows the same downfield shift as for α-2a and is assigned to **7a** (Mes* in β' position), and the other signal is shifted −1.1 ppb and is assigned to **7b** which is located above and in the van der Waals contact with the β-ring. Similarly, β-2a-Me (above and in contact with the α-ring) in **7a** (β' = Mes*) is shifted +0.5 ppb relative to **5**, but in **8a** β-2a moves −1.1 ppb compared to **7a**.

The β-2b-Me site is not influenced by deuteration at α and, in general, the *p*-methyls show little interest in the proceedings. the anomalous sites α-2b and β-2a are just those expected to have strong interactions since they are similarly located in the sterically crowded region between rings α and β.

Significant effects are observed at β'-2a,2b for **8b** compared to **7b** although β'-3a,3b are not influenced. If we assume that negative $\Delta\delta$ values for sites on a [Mes] ring, when another ring becomes [Mes*], reflect a relief of steric interaction, then some tantalizing conclusions can be made. The more stable isotopomer of a pair shows larger negative $\Delta\delta$ values for comparable sites, e.g., at the OH site. In addition, the β-Mes or β'-Mes sites 2a,2b that are CH_3 show more negative $\Delta\delta$ values for **7b** compared to **7a**, **8b** compared to **8a**, and **8** compared to **7**. Sites 3a,3b have direct isotope shift effects as well as steric effects, and the magnitude of these shifts follows the order $\alpha < \beta' < \beta$, which is just the order for $^4J_{3a,3b}$.

Conclusions

The method applied here is based on relative integration of signals and is the simplest used so far for the determination of an equilibrium steric isotope effect. It is capable of measuring relatively small isotope effects but requires a high-field NMR instrument and integration under carefully controlled conditions. These conditions can be met with the newest generation of modern instruments. The method has the advantage that, in contrast to previous determinations where the NMR signals represent average values for two unequally populated rapidly interconverting conformations,[6] the signals used for integration directly represent the two isotopomers under slow exchange conditions. The methyl and OH probes used here measure the same isotopomer ratio in somewhat different ways. The methyl integration determines the population ratio directly for Mes in β and β' positions and this application is not limited to enols. The novelty of the OH probe is that it senses remotely small conformational difference between *E* and *Z* isotopomers caused by the steric differences between Mes and Mes*. Although this observation is presently limited to the two systems under discussion, it may become more general as the use of very high-field NMR spectrometers increases. The main limitation is the presence of lesser deuterated impurity species, but this can be overcome by using precursors of higher purity. The OH probe has the appealing aspect that when the signals are sufficiently separated and species of lesser deuteration are negligible, small effects could be immediately recognized by visual inspection of the heights of the two signals.

Experimental Section

Solvents and Materials. Tetrahydrofuran was distilled from sodium benzophenone ketyl under nitrogen immediately before use. C_6D_6 (99.5% D) was purchased from Merck Sharpe and Dohme and was used without further purification. Compounds **5**,[11b] **7**[12], and **9**[12] were prepared as described previously; compound **12** was prepared by a literature method.[26]

(*E*)- and (*Z*)-2-Mesityl-1,2-bis(2,4,6-trideuteriomethylphenyl)ethenols (8a and 8b). The isotopomeric mixture was prepared by addition of mesitylmagnesium bromide (98.4% D)[11b] in THF to the labeled ketene **6**[12] according to ref 11b. The yield of **8a**/**8b** was 32%.

(*E*)- and (*Z*)-2-Mesityl-2-(2,4,6-trideuteriomethylphenyl)ethenols and the 1-Deutero Derivatives (10a and 10b). The isotopomers were prepared by reduction of the labeled ketene **6** by $LiAlH_4$ or $LiAlD_4$ in THF:[12] mp 115 °C (yield 74%).

(*Z*)-1-Mesityl-2-phenyl-2-(2,4,6-trideuteriomethylphenyl)ethenol (11). The compound was prepared by enolization of 1-mesityl-2-phenyl-2-(2,4,6-trideuteriomethylphenyl)ethanone[27] in 60% yield according to Fuson,[7] mp 136 °C.

NMR Methods. ^1H NMR spectra were obtained with Bruker WH-300, AM-400, and AM-500 FT NMR spectrometers operating at 300.133, 400.134, and 500.135 MHz, respectively. Samples of the substance **5** (4 mg), **7** (4 mg), **8** (4 mg), and **10** (ca. 2 mg) were dissolved in 0.4 mL of C_6D_6 more than 1 h prior to measurement at 500 MHz. The temperature of the samples was actively controlled for all experiments with an equilibration time of at least 30 min, an absolute accuracy of ±1°, and regulation precision of better than 0.1°. Data acquisition parameters for **5** were as follows: spectra width 6024 Hz, time domain 64 K points, acquisition time 5.439 s, relaxation delay 10 s, flip angle 25° (2-μs pulse), ADC-resolution 16-bit, 16 transients. Identical parameters were used for **7** and **8** at 302 K, except the number of transients was 32 for **7** and 64 for **8**. At lower temperatures 64 transients were accumulated. All chemical shifts are reported relative to 7.17 ppm for the residual benzene-d_5 signal. The digital resolution was 0.184 Hz/pt, but the use of zero-filling to 128K points and a cubic interpolation for peak-picking increase the accuracy of frequency measurements to better than ±0.05 Hz (0.1 ppb).

For the purpose of signal assignments **5** was examined at 302 K with spin decoupling difference spectroscopy (SDDS) and NOE difference spectroscopy. Data acquisition parameters for SDDS were: spectral width 4424 Hz, time domain 64K points, acquisition time 7.406 s, relaxation delay 2 s, flip angle ca. 40° (3-μs pulse), 16 transients. The SDDS technique involves steady-state irradiation with a decoupling frequency in the pulsed homonuclear mode. A list of frequencies is prepared for all desired sites of irradiation, e.g., the six aromatic protons, with one frequency value set off-resonance as a control. The control spectrum should represent the unperturbed case since it will be subtracted from each on-resonance case to create the desired difference spectrum. Since SDDS requires irradiation during acquisition, the shift positions of resonances near the decoupling point will be perturbed by the Bloch–Siegert effect. Therefore, the control frequency is placed near the site of on-resonance irradiation, in order to create a similar Bloch–Siegert effect. Even with this precaution and the use of as low a decoupling power as possible, certain shift discrepancies occur, particularly very close to the on-resonance frequency. This can be compensated in localized regions by shifting the control spectrum prior to subtraction. Errors that occur due to the Bloch–Siegert effect result in pure dispersion mode signals with zero total integral. The SDDS spectra presented in Figure 4 were obtained by subtracting the on-resonance spectrum from the control. The irradiated peak then appears as a positive signal which simplifies plotting and integration. The decoupler power used was 30 dB below ca. 0.1 W and ensured complete selectivity.

Decoupling effects in SDDS spectra exhibit themselves as the superposition of a positive normal multiplet and a negative decoupled multiplet. In our case the couplings involved were not resolved (no resolution enhancement) so that the difference spectra showed a sharper negative line with broader positive shoulders (see Figure 4), as expected when decoupling causes a line-narrowing. The amplitude of the negative signal reflects the extent of line-narrowing, i.e., the magnitude of the coupling that is removed.

In addition to decoupling effects the steady-state method generates NOE and/or saturation transfer. In our case these two possibilities could be easily distinguished since the difference spectra show saturation transfer signals with the same sign (positive) as the irradiated site and NOE effects with the opposite sign (negative signals indicate a positive NOE enhancement). The superposition of saturation transfer and decoupling effects produces a positive signal with a pseudo-splitting.

NOE experiments were performed in a manner similar to SDDS except that the decoupler is turned on in CW mode for a presaturation period and off during the acquisition and relaxation delay, eliminating decoupling effects and Bloch–Siegert shifts but not the saturation transfer effects. For the spectra in Figure 5 16K FIDs (48 transients) were acquired with 5 s of presaturation at a power level of 53 dB below 0.1 W. Other experiments were performed with 8-s irradiation at 63 dB attenuation for better selectivity.

The quantitative data of Table II were obtained by integration of the difference spectra, where the irradiated peak integral was defined as 100 for single protons or 300 for methyl groups. The percent saturation transfer or NOE for single protons was given directly by the digital integral values whereas integral values for methyl groups were divided

(25) Anet, F. A. L.; Dekmezian, A. H. *J. Am. Chem. Soc.* **1979**, *101*, 5449.
(26) Biali, S. E.; Rappoport, Z.; Depke, G.; Eckart, K.; Schwarz, H. *Int. J. Mass Spectrom. Ion Proc.* **1985**, *63*, 289.
(27) Fuson, R. C.; Armstrong, L. J.; Kneisley, J. W.; Shenk, W. J. *J. Am. Chem. Soc.* **1944**, *66*, 1464.

by 3 before entering them in Table II.

The spin–lattice relaxation times T_1 were measured by inversion–recovery (90° pulse = 6.8 μs) at 302 K on the same sample (not degassed) used for saturation transfer studies. An equilibration delay of 30 s was used, nine different recovery times, and four transients per FID. Peak heights were fit by nonlinear least-squares analysis to the three-parameter function. $I_z(t) = A - B\exp(-t/T_1)$ to determine A, B, T_1. The values of A and B were 0.97 ± 0.02 and −1.92 ± 0.02, respectively, for all fits.

Resolution enhancement via the Lorentz-to-Gaussion line-shape transformation[28] was used extensively to extract all possible information from the spectra. The natural line width of signals and the relatively broad wings of the Lorentzian line shape normally limit the resolution in NMR spectra. Multiplication of the original free induction decay (FID) with an appropriate double exponential function can remove the Lorentzian component and introduce a narrower Gaussian line shape. Figure 3 shows the result of a rather strong enhancement which has been optimized for the aromatic signals (Figure 3A) to produce a pure Gaussian line shape without wings. For the methyl signals an over-enhancement has been purposely used to clarify the multiplet structure, resulting in a "negative" Lorentzian component giving the negative wings in the spectrum. For integration purposes it is mandatory that the enhancement be performed in such a way as to avoid negative line shapes (Figure 6). The resolution achievable in this way is limited only by the digital resolution and the signal-to-noise ratio in the original FID.

Integration was performed using the computer software routines that allow accurate baseline correction for individual peaks, precise definition of integration limits, and digital printout of integral values. The integrals were normalized either by setting the lowest field aromatic proton or the total OH integral to 1.00. Increasing degrees of resolution enhancement were applied and phase was adjusted by optimizing the flatness and continuity of the baseline across the spectrum. For the OH signal of **7** and **8** some trails were made by dividing the integral in the exact center between the two signals; other trials involving further resolution enhancement allowed impurity peaks to be integrated separately. The results of all trials are summarized in Table III. The integration limits to the left and right of the OH signals were varied from trial to trail to give an indication of the uncertainties involved. The maximum variation that could be produced in a "reasonable" way was ±2%. In general, the methyl signals could be more reproducibly integrated since their line shape was narrower and impurity peaks could be better avoided. Integral tests made with **5** demonstrated conclusively that the integration techniques used can give an absolute accuracy of ±0.005 proton, which is the best one can expect when ^{13}C-satellites cannot be included in each integral.

Acknowledgment. We are indebted to Professor H. Schwarz and to Dr. M. Spraul for preliminary integration experiments and to Professor F. A. L. Anet for discussions. This work was supported by a grant from the United States–Israel Binational Science Foundation (BSF), Jerusalem, Israel, to which we are grateful.

Registry No. 5, 26905-20-4; **7a**, 88180-82-9; **7b**, 88180-83-0; **8a**, 88180-84-1; **8b**, 88200-35-5; **9a**, 88180-86-3; **9b**, 88180-87-4; **10a**, 97571-63-6; **10a**-α-*d*, 97571-64-7; **10b**, 97571-65-8; **10b**-α-*d*, 97571-66-9; **11**, 88180-90-9; **12**, 77787-79-2.

(28) Ernst, R. R. *Adv. Magn. Reson.* **1966**, *2*, 1–135.

Hemiacetal Formation with a Phenol Nucleophile: Simple Proton Transfers as Rate-Limiting Steps

Robert A. McClelland,*† David B. Devine,† and Poul E. Sørensen*‡

Contribution from the Department of Chemistry, University of Toronto, Toronto, Ontario, Canada M5S 1A1, and the Chemistry Department A, The Technical University of Denmark, DK-2800, Lyngby, Denmark. *Received February 4, 1985*

Abstract: A kinetic study is reported of the reversible cyclization in cacodylic acid buffers (pH 5.3–6.5) of (*Z*)-2′-hydroxy-4-methoxy-α-methylchalcone (C) to its cyclic hemiacetal isomer 2-hydroxy-2-(4-methoxyphenyl)-3-methylflav-3-ene (B). Rate–buffer plots for experiments at constant pH exhibit a complex curvature. It is proposed that there are three regions of behavior: very dilute buffers, with a steep increase in rate with increasing buffer concentration; dilute to moderately concentrated buffers, where the rate continues to rise but not nearly so steeply; and very concentrated buffers, where the rate levels. A mechanism is proposed with both the chalcone anion C^- and hemiacetal anion B^- as intermediates $C \rightleftarrows C^- \rightleftarrows B^- \rightleftarrows B$. A kinetic analysis is conducted using the measured equilibrium constant for cyclization, $K = [B]/[C] = 4$, the measured acidity constant for chalcone ionization, $pK_C = 9.1$, and an estimated acidity constant for hemiacetal ionization, $pK_B \approx 12.0$. Consistent with the two breaks in the buffer dilution plots, this analysis establishes that at some buffer concentration each step in the reaction is (mainly) rate limiting, the first step $C \rightleftarrows C^-$ in very dilute buffers, the third step $B^- \rightleftarrows B$ in more concentrated buffers, and the second step $C^- \rightleftarrows B^-$ in very concentrated buffers. The proton-transfer steps are rate limiting in dilute buffers because the anion equilibration is extremely rapid. The changes in the rate-limiting step arise because of the acceleration of the proton transfers due to participation of the buffer. A comparison with the formation/breakdown of other hemiacetals is presented. The principal difference of the chalcone system is the uncoupling of both proton transfers from C–O bond making or breaking. The factor responsible for this appears to be the increased stability of the phenoxide nucleophile/leaving group.

Several recent investigations have provided evidence[1-3] for a class "n" mechanism[4] in the general-base-catalyzed[5] addition of water and alcohols to aldehydes (eq 1). This involves, in the addition direction, a proton transfer from the water or alcohol nucleophile to the catalyzing base coupled with C–O bond formation. The second proton transfer, which is required for the

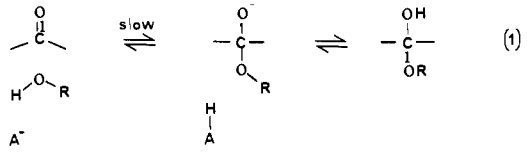

(1)

† University of Toronto.
‡ The Technical University of Denmark.

(1) Funderburk, L. H.; Aldwin, L.; Jencks, W. P. *J. Am. Chem. Soc.* **1978**, *100*, 5444–5459.
(2) McClelland, R. A.; Coe, M. *J. Am. Chem. Soc.* **1983**, *105*, 2719–2725.
(3) Sørensen, P. E.; Jencks, W. P. *J. Am. Chem. Soc.*, submitted.
(4) Jencks, W. P. *Acc. Chem. Res.* **1976**, *9*, 425–432.
(5) Bell, R. P. *Adv. Phys. Org. Chem.* **1966**, *4*, 1–29.
(6) (a) Hemiacetals and hydrates are more acidic than simple alcohols[6b] because of the acid-strengthening effect of the additional oxygen atom present in the former. (b) Hine, J.; Koser, G. F. *J. Org. Chem.* **1971**, *36*, 1348–1351.

0002-7863/85/1507-5459$01.50/0